DEVELOPMENT OF STIFFNESS EVALUATION SYSTEM THAT CONSIDERS MOLDING-INDUCED LONG-FIBER WAVINESS USING NUMERICAL SIMULATIONS

Masatoshi Kobayashi, Koji Dan
Automobile R&D Center, Honda R&D Co., Ltd.
Takuya Uenoyama, Motoharu Tateishi
Sales Operation, MSC Software Co., Ltd.

Abstract

In this study, a 3D coupled simulation (co-simulation) system with molding and structural analyses has been developed in order to evaluate the influence on local stiffness by long-fiber waviness that occurs during compression molding. For the molding analyses, the cavity filling behavior was computed using the finite volume method (FVM) and long-fiber motions were computed successively using the direct long-fiber simulation (DFS) method. After that, arbitrary representative volume elements (RVE), which were extracted from a mesh model for the molding analyses, were remodeled for structural analysis. Then, for the structural analysis, local stiffness in molded parts was simulated using the finite element method (FEM), with long-fibers modeled directly using the computational results of the long-fiber motion. The co-simulation results indicate that the long-fiber waviness state induced by molding differs locally and that stiffness is influenced by the degree of long-fiber waviness.

Introduction

For the purpose of vehicle weight reduction, discontinuous long-fiber reinforced thermoplastics (LFT) which have high stiffness and high strength have been applied to body parts in the automobile industry. Thermoplastics with long-fiber (a few mm to 50 mm in length) reinforcements are typically used in the compression molding. Basically, in order to increase the stiffness and strength as much as possible, reinforcement fibers and molding conditions are chosen so that longer fibers can remain in the molded parts. By contrast, long-fiber waviness induced by resin flow is more likely to occur in molded parts since the flexibility of the fiber increases as the fiber length increases. As you well known, flow-induced fiber conditions, such as fiber orientation and fiber ratio, significantly influence as-manufactured mechanical properties. LFT parts have complex anisotropy distribution of the mechanical properties, because these conditions differ locally. In the case of long-fibers, another characteristic fiber condition is waviness. Although the waviness is presumed to also influence the mechanical properties, the relationship between long-fiber waviness and mechanical properties has seldom been discussed [1, 2]. The reason for this lack of discussion is that long-fiber waviness conditions in LFT specimens are not easy to understand sufficiently using experimental methods, even with the use of micro X-ray computed tomography (X-CT) equipment. For reference, some of the authors of this paper have reported that long-fiber waviness might cause Young's modulus and tensile strength to decrease. They found out this by comparing one LFT specimen in which significant long-fiber waviness was observed and another LFT specimen in which such waviness was not observed, using a microscope, to view two-dimensional cross-section surfaces [2].

On the other hand, numerical simulation technologies have evolved significantly in recent years. In molding simulations, direct long-fiber simulation (DFS) using a large number of long-fiber models has been recently developed by some of the authors and collaborators [2-4]. The long-fiber waviness distribution in entire LFT parts can be broadly predicted using this DFS. In a structural simulation, the computations for elements in which both resin and fiber regions are present can be roughly divided into two methods. These are the mean-field homogenization method [5, 6], in which the elements are given average property values, and the localization method, in which the elements are given average deformation amounts. However, there are very few reports on structural simulation considering the influence of long-fiber waviness. In particular, there may be no reports on co-simulation with molding and structural analyses that consider the influence of long-fiber waviness.

This paper discusses the possibility of an as-manufactured local stiffness evaluation for LFT by 3D co-simulation using long-fibers modeled directly, in both molding simulations and structural simulations. For reference, the localization method was applied here. The results indicate that it was possible to evaluate local stiffness influenced by molding.

Co-Simulation Method

Figure 1 shows the co-simulations procedure for an as-manufactured local stiffness evaluation. This co-simulation consists of three different computations and is performed in the order cavity filling computation, long-fiber motion computation, and small-scale stiffness computation using long-fibers modeled directly. In addition, in order to use output data from long-fiber motion computations as input data for small-scale stiffness computations, this procedure also requires a mesh mapping process to convert arbitrary representative volume elements extracted from a mesh model for a molding simulation into different elements for a structural simulation.

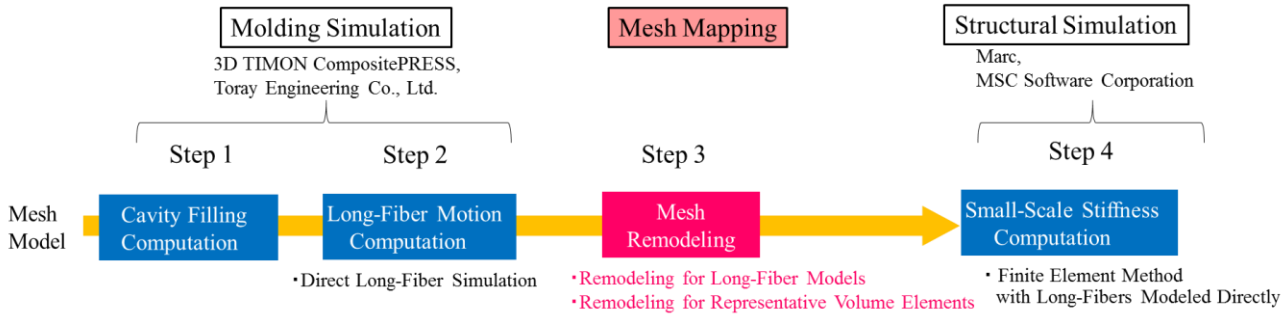

Figure 1: 3D co-simulation flow diagram

Therefore, authors have developed a mesh mapping system for remodeling both the elements extracted from the molding simulation result and long-fiber models contained in these elements. The details of the co-simulation method are described below.

Input material properties

As material properties, discontinuous glass long-fiber reinforced polyamide 6 sheets (hereinafter referred to as LFT sheets) with a fiber volume ratio of 45% is assumed. First, as the

properties for molding simulations, Table 1 shows the measured values of thermal conductivity, specific heat, and density. These are simplistically treated as constant values. Table 2 shows a shear viscosity model [4], which selects from viscosity equations with different coefficients for each temperature range, and their coefficient values. This viscosity model is called the multiple 3-constant-Arrhenius model. Some of the authors have reported that this viscosity model was in good agreement with measured values over a wide shear rate range and a wide temperature range [4]. Next, as properties for structural simulation, Table 3 shows Young's modulus and Poisson's ratio of the resin and long-fibers, respectively.

Table 1: Material properties for molding simulations

Material data		
Thermal conductivity (W/m K)	Specific heat (J/kg K)	Density (kg/m3)
0.2	1400	1300

Table 2: Viscosity model [4] and its coefficients for molding simulations

Shear viscosity								
High temperature region More than 205 ℃ $\eta_s = A_1 \dot{\gamma}_s^{B1} exp(C_1 \cdot T)$			Transition temperature region Between 205 and 192 ℃ $\eta_s = A_2 \dot{\gamma}_s^{B2} exp(C_2 \cdot T)$			Low temperature region Less than 192 ℃ $\eta_s = A_3 \dot{\gamma}_s^{B3} exp(C_3 \cdot T)$		
A_1	B_1	C_1	A_2	B_2	C_2	A_3	B_3	C_3
2.5E7	-0.8	-0.02	3.0E41	-0.78	-0.40	9.0E8	-0.95	-0.01

η_s: Shear viscosity (Pa·s)
$\dot{\gamma}_s$: Shear rate (s^{-1})
T : Material temperature (℃)

Table 3: Material properties [7, 8] for structural simulations

Material data		
Material type	Poisson ratio	Young's modulus (GPa)
Matrix resin	0.39	3.2
Long fibers	0.23	80

Part shape model

Figure 2 shows the shape model that is used for the molding simulation, and which is determined by referring to the partial shape of an automobile part. This is a hat-shaped model

with thickness changes; it has a thin section, a stepped section, and a thick section in both the top and sloped surfaces.

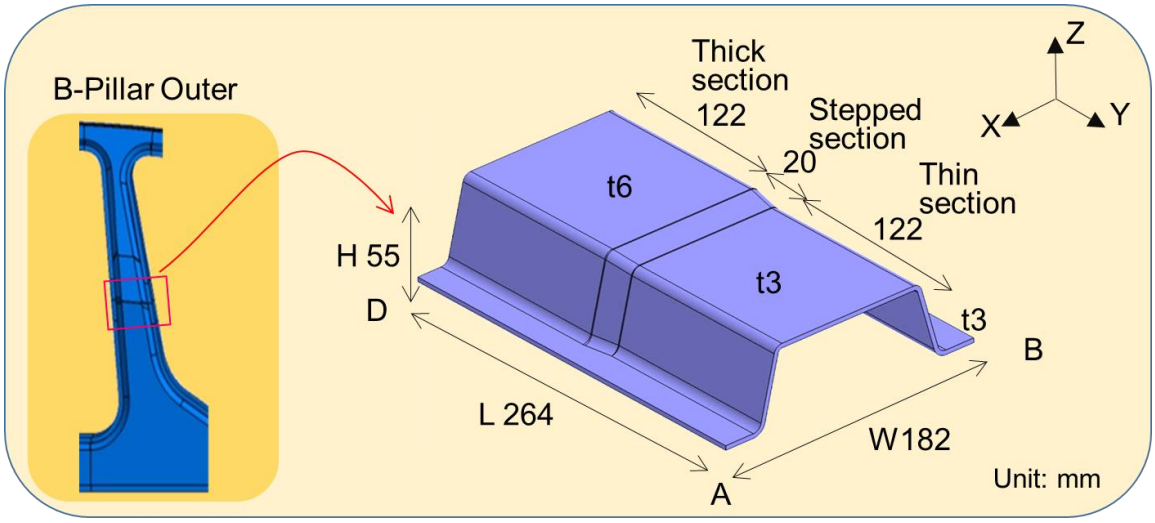

Figure 2: Part shape dimensions for molding simulations

Molding simulations

The following methods are used for mold a cavity filling computation for compression molding. A commercial software program was modified so that the LFT melt flow could be simulated using the multiple 3-constant-Arrhenius model.

- Software: Modified 3D TIMON-CompositePRESS (Toray Engineering Co., Ltd.)
- Flow computation method: The finite volume method (FVM)
- Fluid Model: Non-isothermal and incompressible non-Newtonian
- Elements: Hexahedrons (including any hexahedrons other than regular hexahedrons)
- Reference frame: Eulerian method
- Fiber motion computation method: Direct long-fiber simulation(DFS)

Table 4: Molding conditions for molding simulations

Compression molding			
Initial material temperature (℃)	Mold temperature (℃)	Heat-transfer coefficient between material and mold (W/m^2K)	Compression speed (mm/sec)
270	180	1000	3.5

First, a three-dimensional mesh model for the initial mold cavity is created. Specifically, the distance between the upper mold surface and the lower mold surface is set to be larger than the thickness of the hat-shaped model, and hexahedral elements are arranged between the mold surfaces. These elements for the initial LFT melt sheets are assigned for each range up to 3 mm from the lower mold surface (thin section) and up to 6.5 mm from the lower mold surface (thick section). In consideration of both analysis accuracy and computational efficiency, fine elements are arranged on the lower mold side and relatively coarse elements are arranged on the upper mold side. Then the LFT melt flow is computed using the molding conditions shown in Table 4. Downward movement of the upper mold is controlled by compression speed.

Figure 3 schematically shows a flexible long-fiber model placed in a flow field for the direct long-fiber simulation (DFS). Now, the long-fiber model, which consists of multiple rigid rods and hinge nodes, is examined. The long-fiber motions are assumed as follows.

- Fiber mass, bending, and torsional moment can be ignored.
- Fiber-fiber interactions can be ignored.
- Fiber movements depend on fluid force acting only at each hinge node.
- The distance between the hinge nodes (rod length) is maintained.

A large number of long-fiber motions are simulated using the result of the cavity filling computation. Table 5 shows the generation conditions of the long-fiber models. Some of the authors have reported detailed equations [2]. These are described briefly as follows. First, each hinge node is temporarily moved by the fluid force. Immediately after the movement, all node positions are adjusted for fixing the distance between adjacent nodes constant. This is repeated for each node of all long-fiber models for each time interval Δt. This procedure is performed simultaneously and continuously for all hinge nodes of all long-fiber models until flow stops.

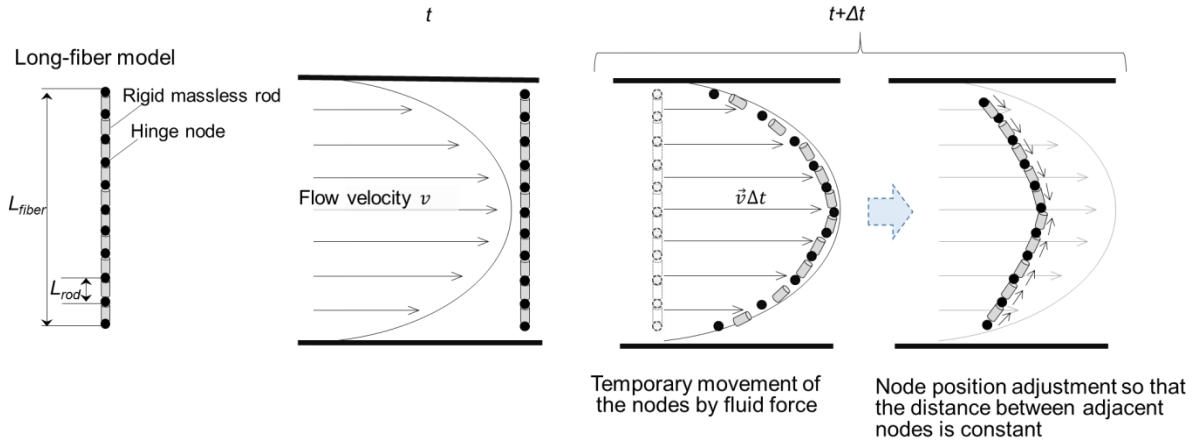

Figure 3: Schematic diagram of a direct long-fiber simulation method

Table 5: Generation conditions for long-fiber models

Long-fiber model					
Long-fiber length L_{fiber} (mm)	Rod length L_{rod} (mm)	Number of hinge nodes per long fiber	Number of long fibers	Initial orientation	Initial waviness
20	2	11	4363	In-plane random orientation	Straight only

Mesh mapping

Authors developed a mesh mapping system, in order to create elements for computing small-scale as-manufactured local stiffness. This system can remodel elements extracted from a mesh model for molding simulations into elements for a structural simulation. This procedure is described below.

First, as representative volumes to be evaluated for local stiffness, hexahedral elements including the nodes of long-fiber models are extracted from an arbitrary position in a hat-shaped mesh model after the molding simulation. Next, these elements are remodeled into finer sized voxel elements for structural analysis, while the total volume remains constant. Then, three-dimensional long-fiber shape models are created using each coordinate point at the nodes of the long-fiber models included in these representative volumes. The positions of these long-fiber shape models and the voxel elements are compared, and each element is assigned to one of either "resin region", "fiber region", or "resin-fiber coexistence region" as shown in Figure 4. Table 6 shows the remodel condition.

Due to the problem of the computation efficiency in the DFS, it is difficult to simulate these motions using the same number of long-fiber models as actual LFT sheets. Therefore, although the co-simulation is performed with fewer long-fiber models than there actually are, the long-fiber diameter is increased virtually to more than the actual number through this mapping, in order to sufficiently provide the fiber influence on the voxel elements.

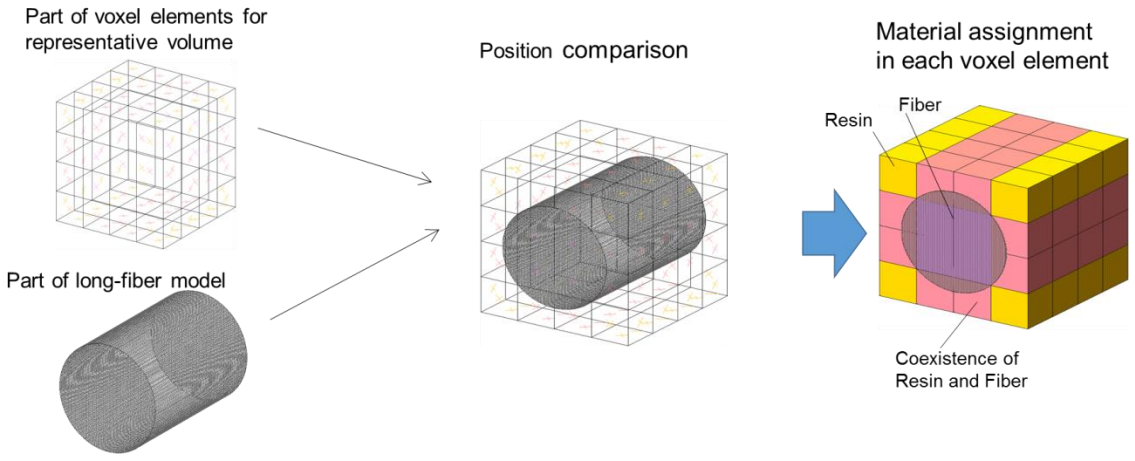

Figure 4: Schematic diagram of material type assignment to voxel elements in mesh mapping

Table 6: Representative volume voxel element and deformation condition for structural simulation

Remodeled mesh and strain				
Diameter of long fibers (mm)	Dimension of representative volume (mm)	Dimension of voxel element (mm)	Applied strain	
			Tensile strain	Shear strain
0.3	5 x 5 x 3	0.05 x 0.05 x 0.05	X direction: 0.01 Y direction: 0.01 Z direction: 0.01	XY direction: 0.01 YZ direction: 0.01 ZX direction: 0.01

Structural simulation

The following methods are applied for structural simulation.

- Software: Marc (MSC Software Co., Ltd.)
- Deformation calculation method: Linear analysis by the finite element method (FEM)
- Solid material model: Linear elastic body
- Elements: Voxel (regular hexahedron only)
- Reference frame: Lagrangian method

Here, in each voxel element, stiffness matrix is calculated using the material properties shown in Table 3, under the assumption of isotropic materials. For elements of the "resin-fiber coexisting region", the following two methods are applied. In method A, a fiber volume ratio V of 50% is assumed for the elements simplistically. In method B, each fiber volume ratio V is calculated for the elements respectively. After that, the stiffness matrix and the compliance matrix dependent on the V are calculated using equation (1). The elastic modulus and Poisson ratio in the elements are obtained from components of the compliance matrix.

$$\boldsymbol{K}_{coexistence} = V\boldsymbol{K}_{fiber} + (1-V)\boldsymbol{K}_{resin} \quad (1)$$

where $\boldsymbol{K}_{coexistence}$ is the stiffness matrix for the resin-fiber coexisting region, $\boldsymbol{K}_{fiber}$ is the stiffness matrix for the fiber region, and $\boldsymbol{K}_{resin}$ is the stiffness matrix for the resin region.

With regard to the whole representative volume voxel elements, the stiffness matrix and the compliance matrix are computed using the deformation conditions shown in Table 6, under the assumption of orthotropic materials. Through these procedures, the tensile elastic modulus E 11 in the X direction of the whole representative volume voxel elements is simulated.

Results and Discussion

Below are the co-simulation results for local stiffness to be carried out in consideration of long-fiber waviness induced by compression molding.

Molding simulation

Figure 5 (a) shows the computation result for resin pressure distribution by color contour when the mold is filled. The upper mold stopped after approximately 0.25 seconds after contacting the fluid. At this time, the cavity was completely filled with the fluid. The pressure indicated the maximum value near the stepped section of the top surface. Figure 5 (b) shows the computation result for the long-fiber motions when the mold is filled. The many long-fibers, which were straight before the flow, moved due to the resin flow and their shapes changed. In addition, the many long-fiber shapes were different depending on their positions. This was caused by differences in the movement of each node of the long-fiber models because different flow velocity distributions occurred depending on position.

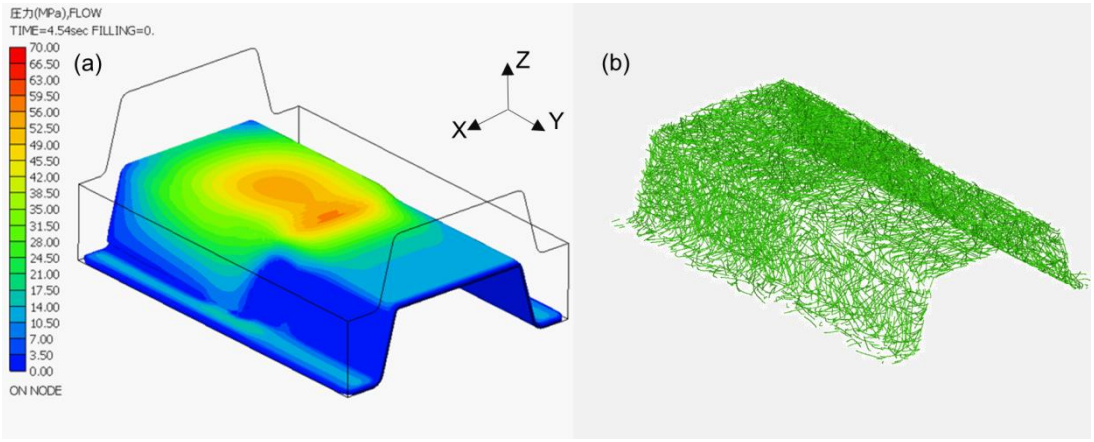

Figure 5: Final filling pattern using the compression molding simulation. (a) resin pressure (b) long-fiber behavior

Mesh mapping

Representative volumes were extracted one by one from arbitrary positions in the thin section and the thick section of the top surface, using the molding simulation results. As a result, one volume from the thin section contained long-fibers with smaller waviness, while the other volume from the thick section contained long-fibers with larger waviness.

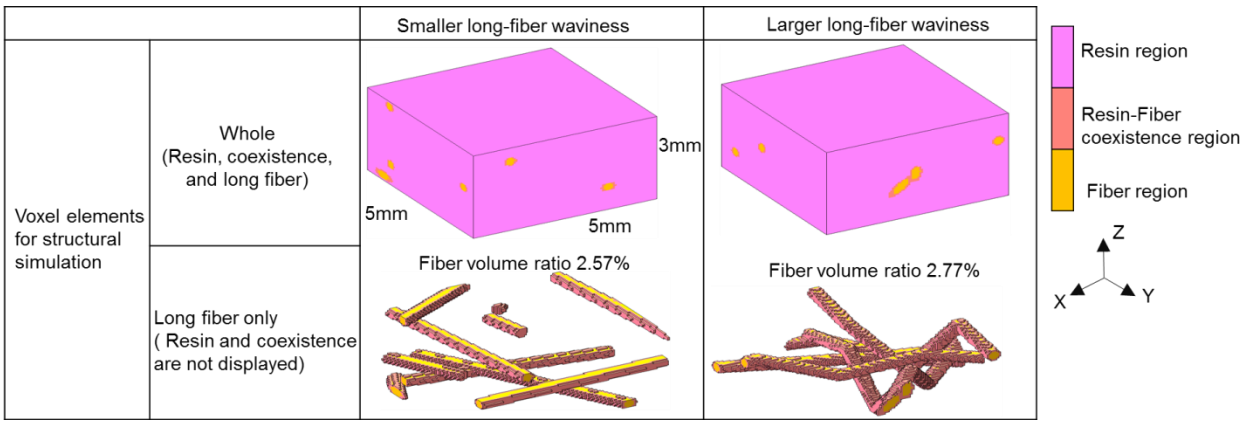

Figure 6: Voxel elements created from representative volumes extracted from arbitrary positions in the molding simulation result using the developed mesh mapping system

The developed mesh mapping system was able to create remodeled voxel elements, including the representative volumes and the long-fiber data. Then, each voxel element was also able to be assigned to a "resin region", "fiber region", or "resin-fiber coexistence region". That is to say, it was possible to complete the mesh mapping. Figure 6 shows the two voxel element models created. Although these models had almost the same fiber volume ratio, the degree of long-fiber waviness differed.

Structural simulation

Since element size influences computation results, the elastic modulus E11 in the whole representative volume voxel elements was computed beforehand using different element sizes. As a result, the element size was narrowed to 0.05 mm in length per side. Figure 7 shows the computed values of E11 in the two voxel element models, using the method A which a fiber volume ratio of 50% was assumed for each element of the "resin-fiber coexisting region". E11 for the element model, which included the larger long-fiber waviness, was lower than that of the element model, which included the smaller long-fiber waviness. E11 computed using the method B, which each fiber volume ratio V is calculated for the elements of the "resin-fiber coexisting region", showed the same tendency as the results using the method A. In other words, this co-simulation predicted that the waviness would influence local stiffness.

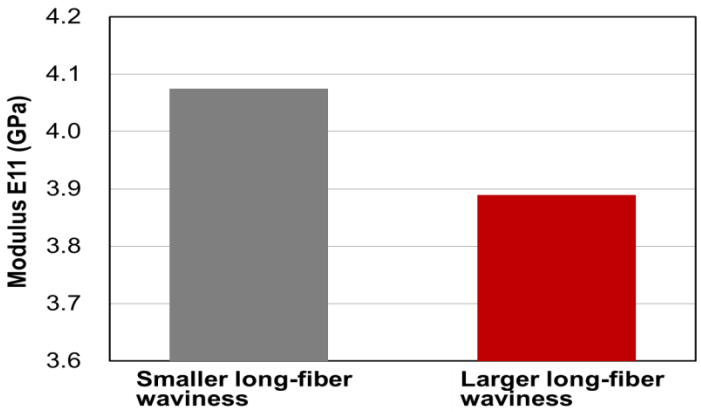

Figure 7: Influence of long-fiber waviness on local stiffness in the whole representative volume voxel elements using the method A

Summary and Next Steps

Authors established a co-simulation system for evaluating local stiffness that considers long-fiber waviness induced by compression molding. The partial hexahedron mesh models for the molding simulations, which were extracted as two arbitrary representative volumes that include the long-fibers, were able to be remodeled to the voxel element models for structural analysis by using the developed mapping system. After that, each voxel element was assigned to either a "resin region", "fiber region", or "resin-fiber coexistence region". The co-simulation that applies strain to these voxel mesh models indicates that local stiffness is influenced by the degree of long-fiber waviness.

Currently, authors are beginning to study the waviness influence on elastic modulus

components other than E11 in this voxel model. In the future, the influence of waviness due to long-fibers with a higher elastic modulus will also be simulated. In addition, this co-simulation system will be extended to local strength evaluation in the long term.

Acknowledgments

Authors would like to thank Mr. Daisuke Urakami (Toray Engineering Co., Ltd.) for supporting the molding analyses.

Bibliography

1. Kunc, V., S. W. Case, H. J. Santos-Villalobos, & S. Simunovic, “The Stiffness Tensor for Composites with Curved Discontinuous Fibers,” Composites Part A: Applied Science and Manufacturing, Vol.72, pp.239-248, 2015.
2. Kobayashi, M., K. Dan, D. Urakami & R. Nakano, “Direct Simulation for Flexible Long-Fiber in Compression Molding of Thermoplastic Composite,” Proceedings of 15th Japan International SAMPE Symposium and Exhibition (JISSE15), 27-29 November, 2017, Tokyo, Japan.
3. Nakano, R. & K. Sakaba, “Development of CAE Software for Injection and BMC/SMC Molding Including Short/Long Fibers Reinforcement,” Proceedings of SAMPE Tech, 2-5 June, 2014, Seattle.
4. Kobayashi, M., K. Dan, T. Baba & D. Urakami, “Compression Molding 3D-CAE of Discontinuous Long Fiber Reinforced Polyamide 6: Influence on Cavity Filling and Direct Fiber Simulations of Viscosity Fitting Methods,” Proceedings of 20th International Conference on Composite Materials, Process Modelling 4, 19-24th July, 2015, Copenhagen, Denmark.
5. Terada, K., “Numerical Characterization of Composite Materials by the Homogenization Method,” Journal of the Japan Society of Polymer Processing, Vol.29, No.2, pp. 42-46, 2017.
6. Kikuchi, N., “Homogenization Method and its Application to Material Design for Composites”, Proceedings of Int. Conf. Comput.-Assist. Mater. Des. Process Simul., pp. 434-439, 1993, Tokyo, Japan.
7. Goto, K., “Temperature Dependence of Elastic Modulus of FRP Glass Fibers,” Journal of Materials Science, Japan Vol.42, No.475, pp.355-358, 1993.
8. Balana, B., & M. Achintha, “Experimental and Numerical Investigation of Float Glass–GFRP Hybrid Beams,” Proceedings of Challenging Glass 5 Conference on Architectural and Structural Applications of Glass, June, 2016, Ghent University.